

Assessment of Sustainable Urban Expansion with Land Use and Land Cover Changes for Al-Hillah City Using Remote Sensing and GIS Techniques

Saif S. Saud^{1a*}, Sundus A. Abdullah^{1b} and Bassim M. Hashim^{2c}

¹Department of Remote Sensing and GIS, College of Science, University of Baghdad, Iraq

²Environment and Water Directorate, Ministry of Science and Technology, Iraq

^bE-mail: sundusalbakri70@gmail.com, ^cE-mail: bassim_saa22@yahoo.com

*Corresponding author: saif.saud2109m@sc.uobaghdad.edu.iq

Abstract

The current study used satellite data and a geographic information system (GIS) to detect changes in land use and land cover (LULC) in Al-Hillah city, central Iraq from 1990 to 2022. The study aimed to calculate the NDVI, NDWI and LULC of Al-Hillah using Landsat 5 TM and Landsat 8 OLI images. The results showed that there was an apparent expansion in the urban area from 20.5 km² in 1990 to about 57 km² in 2022. On the other hand, there is a slight increase in agricultural areas and water, while the barren area decreased from 168.7 km² to 122 km² in 2022. Long-term urban planning, which is based on LULC analysis, is an effective tool for decision-makers to study future patterns in urban expansion in parallel with the expected rise of the population in Iraq in the coming years. While there was a slight increase in water and agricultural areas. The continuous urban expansion led to a reduction in barren areas in favor of urban areas. Urban planning for a long period, which is based on LULC analysis, where demographic changes greatly affected land use in the city of Al-Hillah, and the increase appears significantly in the urban and residential areas.

Article Info.

Keywords:

Urban Expansion, Land Use, Land Cover, GIS, Landsat Data.

Article history:

Received: Jun. 21, 2023

Revised: Aug. 29, 2023

Accepted: Sep. 03, 2023

Published: Dec. 01, 2023

1. Introduction

The creation of land use and land cover (LULC) maps is one of the most significant applications of remote sensing and geographic information system (GIS). Land use is the term used to describe the objectives of a land survey, encompassing tourism, animal habitat protection, agriculture, urban development, and the majority of areas where humans have an effect. Whether it is vegetation, water, bare soil, urban development, or anything else, land cover refers to the surface cover [1, 2]. As a result of changes in the earth's surface and urbanization (land cover), this study relied on the criteria of the thematic strata factor for land use, land cover types, built-up areas, and green spaces [3, 4]. Land cover originally refers to the physical state of the earth's surface, the variety of the soil, the surface and ground waters and the soil type land use. On the other hand, describes how people use land and its resources, such as via agriculture, urban growth, pastoralism, logging, and mining [5-7]. However, the definition of LULC is the replacement of one form of LC on the earth's surface with another [8]. Using Landsat images to record the spatiotemporal pattern of LULC, researchers can identify the factors that influence changes in human activity patterns as well as their causes [9, 10]. LULC in Iraq and its changes have a significant impact on the natural environment and economic activities of humans. The surface vegetation index is an important indicator for monitoring global changes. Therefore, many researchers have focused on the type of canopy and the distribution and diversity of plants and trees. At the same time, the vegetation index can also be used to assess environmental issues, such as crop products, land cover assessments or land-use surveys [11, 12]. Detecting changes in LULC and keeping track of interactions between natural

phenomena and human endeavors are both made possible by optical remote sensing (RS) [13, 14]. Additionally, RS reduces prices, energy use, and time. RS optical data is now often employed to identify LULC dynamics, including satellite sensor pictures and aerial photography. The results of LULC mapping are utilized for leading landscape scales, change detection, global, regional, and local mapping. It is possible to think of the categorization of remote sensing images as a collaborative endeavor between technologies for image processing and classification [15, 16]. A key method in the quantitative analysis of remotely sensed images is multispectral image categorization. Typically, a pixel (image element) from a multispectral image has its attributes captured on many spectral channels [17, 18].

There is a previous study dealing assessing land use in Al-Hillah (Zahraa Abbas and Hussein Sabah Jaber, 2020) [19], (Mohammed Irzoqy, I.M., Ibrahim, L.F. and Al-Tufaily, H.M.A., 2022, March) [20], (Fahad, K.H., Hussein, S. and Dibs, H., 2020) [21].

The extraction of data from remote sensing includes the classification of images. This research aims to calculate: i) Normalize difference vegetation index (NDVI); ii) Normalize difference water index (NDWI); and iii) Supervised classification of LULC from 1990-2022 in Al-Hillah city.

1.1. Study Area

The current study area was conducted in Al-Hillah district, located at 32° 28' 46" north and 44° 25' 58" east. Al-Hillah its full original name, and has a total area of 270 km². Its land slopes towards the south rise 35 m above sea level. A desert climate prevails which is characterized by low rainfall and high temperatures in summer and reach 50°C, and whereas a warm climate prevails in winter. Al-Hillah has a population of about 317,835 [22], which is in the shape of a square or rectangle as shown in Fig. 1.

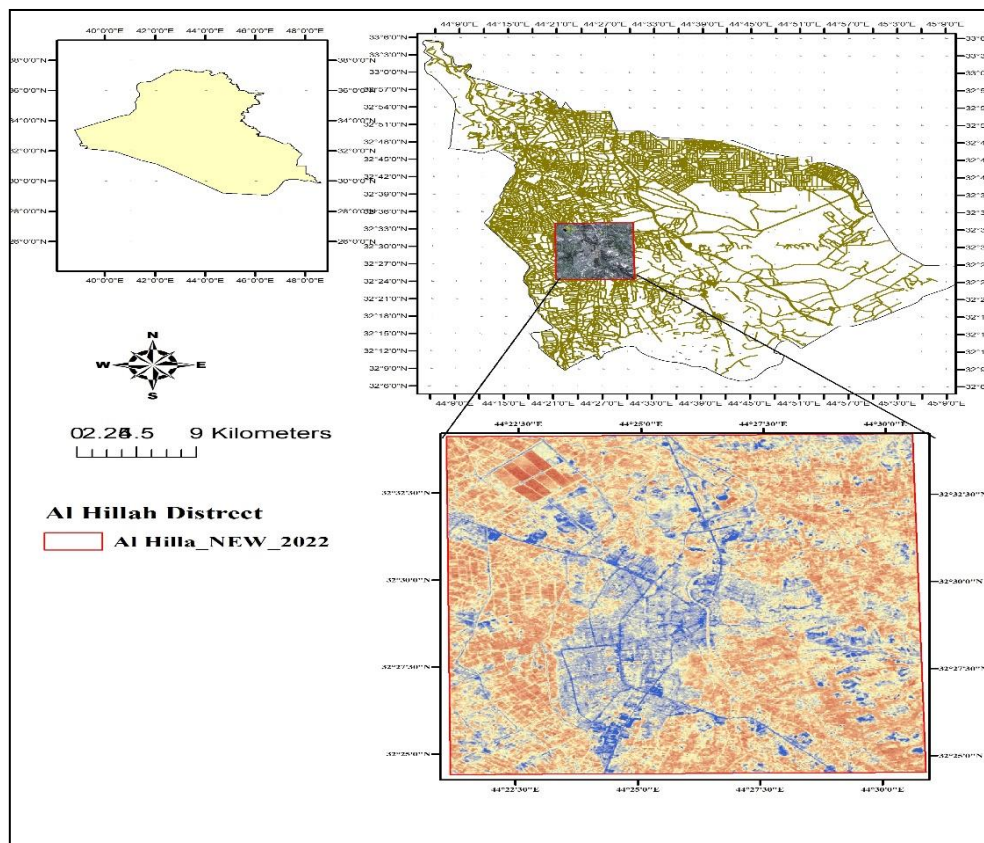


Figure 1: Location of the Study area.

1.2. Data Sources

The Landsat images of Al-Hillah acquired in January during the clear and rainy weather and used in the current investigation. These images are available on the USGS website, Earth Explorer [23, 24]. The Landsat 5 images were acquired on January 8 of 1990, 2000 and 2010 as shown in Table 1, while Landsat 8 images were acquired on January 8, 2022, as illustrated in Table 2.

Table 1 Landsat 5 bands.

Band No.	Wavelength (μm)	Spatial Resolution (m)	Bands
1	0.45 - 0.52	30	Blue
2	0.52 - 0.60	30	Green
3	0.63 - 0.69	30	Red
4	0.77 - 0.90	30	NIR
5	1.55 - 1.75	30	MIR
6	10.40 - 12.50	30	Thermal
7	2.09 - 2.35	30	MIR

Table 2 Bands of Landsat 8 OLI.

Band No.	Wavelength (μm)	Spatial Resolution (m)	Bands
1	0.43 - 0.45	30	Coastal
2	0.45 - 0.51	30	Blue
3	0.53 - 0.59	30	Green
4	0.63 - 0.67	30	Red
5	0.85 - 0.88	30	NIR
6	1.57 - 1.65	30	SWIR 1
7	2.11 - 2.29	30	SWIR 2
8	0.50 - 0.68	15	Pan
9	1.36 - 1.38	30	Cirrus
10	10.60 - 10.19	100	TIRS 1
11	10.50 - 12.51	100	TIRS 2

The atmospheric modifications made to the Landsat images that were used in this investigation improved the image quality and decreased noise [25, 26]. The images were compatible with Landsat 8 images since they feature bands with a resolution of 30 m [27].

2. Classification Techniques

Each pixel in the image or the original remotely sensed satellite data is classified according to its kind in a process known as "classification", which aims to produce a good collection of land cover information. Based on the various land features, the classification is influenced by the studied region's (rural or urban) nature, which makes each spectral category unique. A classification differs for each single species through its unique reflectance and diffusion characteristics. Modern classification techniques, including supervised and unsupervised methods, are commonly used to produce land cover maps [28, 29].

2.1. Supervised Classification

A form of machine learning known as supervised classification uses predetermined training samples and a classification algorithm. The classification algorithm often used in supervised remote sensing is the classification process [30]. The supervised part is the most compelling portion of the Landsat image categorization technique and is the sample for training [31]. The accuracy categorization is strongly

reliant on the training samples chosen; when you are done with this; you will have a finished product. The categorization accuracy is strongly dependent on the selected training examples. A classification is given to every class, which the business refers to as training [32]. The classification accuracy assessment is very important in land use mapping and understanding map quality and reliability [33]. In supervised categorization, the user must pick a region of interest. This will serve as a classifier in the image [34]. All pixels in the image will be utilized. The quality of the supervised categorization is based on the caliber of the training locations [35, 36].

3. Methodology

There were two primary phases in the current study. The initial phase involved classifying satellite data according to LULC. The second phase centered on the examination of this change detection in the LULC values. The satellite data analysis includes registration, categorization, and change detection using post organization comparative satellite data [37, 38]. The area under study is depicted by a Landsat image that was chosen for the study period (1990, 2000, 2010, and 2022) from Landsat 5 TM, and Landsat 8 OLI running utilizing various sensors and data acquired from USGS Earth Explorer for thirty years with the aim of mulching during the drying season and environmental effects in Al-Hillah. Images reserved at Al-Hillah during the drying process and its effects on the environment are clear of clouds, (Distortions brought on by the intervening atmospheric conditions), haze, and dust. The images were processed and interpreted to create LULC using the imagine application (ArcGIS 10.5) [39, 40]. To identify the change in land cover, the conducted data were retrieved, examined, and estimated. Forecasting prospects was based on data from the past.

3.1. Specification Indices

3.1.1. Normalize Difference Vegetation Index (NDVI)

Each Landsat image has its own normalize difference vegetation index (NDVI) calculation. Healthy vegetation is an excellent electromagnetic spectrum absorber for a clear reason [41]. Chlorophyll is a substance found in greenery that powerfully reflects green (0.5-0.6 μm), red (0.4-0.5 μm), and blue (0.4-0.5 μm) [42, 43]. So, a vegetation appears in our eyes as green. Plants that are solid and have a long near IR (NIR) reflectivity around 0.7-1.3 μm [44, 45]. A plant's interior structure frequently plays a part in this. High Ruddy retention and long NIR reflectance are the two criteria used to determine the NDVI [46, 47]. NDVI is calculated using the formula below. NDVI is calculated based on Eq. (1):

$$\text{NDVI} = \frac{\text{NIR} - \text{R}}{\text{NIR} + \text{R}} \quad (1)$$

The NDVI value is in the range of -1 to 1. Higher NDVI readings represent greater NIR levels, which suggest thick vegetation.

3.1.2. Normalize Difference Water Index (NDWI)

For the examination of the water bodies, the normalized difference water index (NDWI) is used [48]. Green and NIR bands of further discovered images were used in the index. In most instances, the NDWI can effectively enhance water data. Building on land while producing valuable water bodies is tricky [49]. To survey the configuration of clear, alter zones, the NDWI items can used in combination with the NDWI alter items. Water bodies can reflect more light. A definite portion of the electromagnetic wave range contained reflections. The majority of time, water bodies have higher blue

(0.4-0.5 m) than green (0.5-0.6 m) and ruddy (0.6-0.7 m) reflectance, while they are in their fluid condition [50].

NDWI is calculated by Eq. (2) from the difference between green short-wave infrared (SWIR) according to Xu (2005) [51]:

$$NDWI = \frac{(NIR - SWIR)}{NIR + SWIR} \tag{2}$$

The clear water has the strongest reflection in the blue portion of the distinct range. The water appears blue. The NDWI value ranges from -1 to 1. Water bodies' NDWI value is more than 0.5. Compared to correctly distinguishing trees from water bodies, plants have substantially lower values. Positive build-up highlights have values between 0 and 0.2.

4. Results

4.1. NDVI

Estimated NDVI values for the city of Al-Hillah for the years 1990, 2000, 2010 and 2022 were based on Landsat images. Fig. 2 shows the NDVI values for Al-Hillah city estimated from Landsat 5 images in 1990 between 0.649 and -0.55. Most of the areas of Al-Hillah were covered with palm groves and farms, especially on both sides of the Euphrates River, which led to a wide coverage, represented by a high NDVI close of 0.65. Because the Greenland regions were due to the lack of large urban and residential areas, so the values of agricultural areas became large and wide.

In 2000, the NDVI scale of the Landsat 5 image was between (0.70 - 0.60).

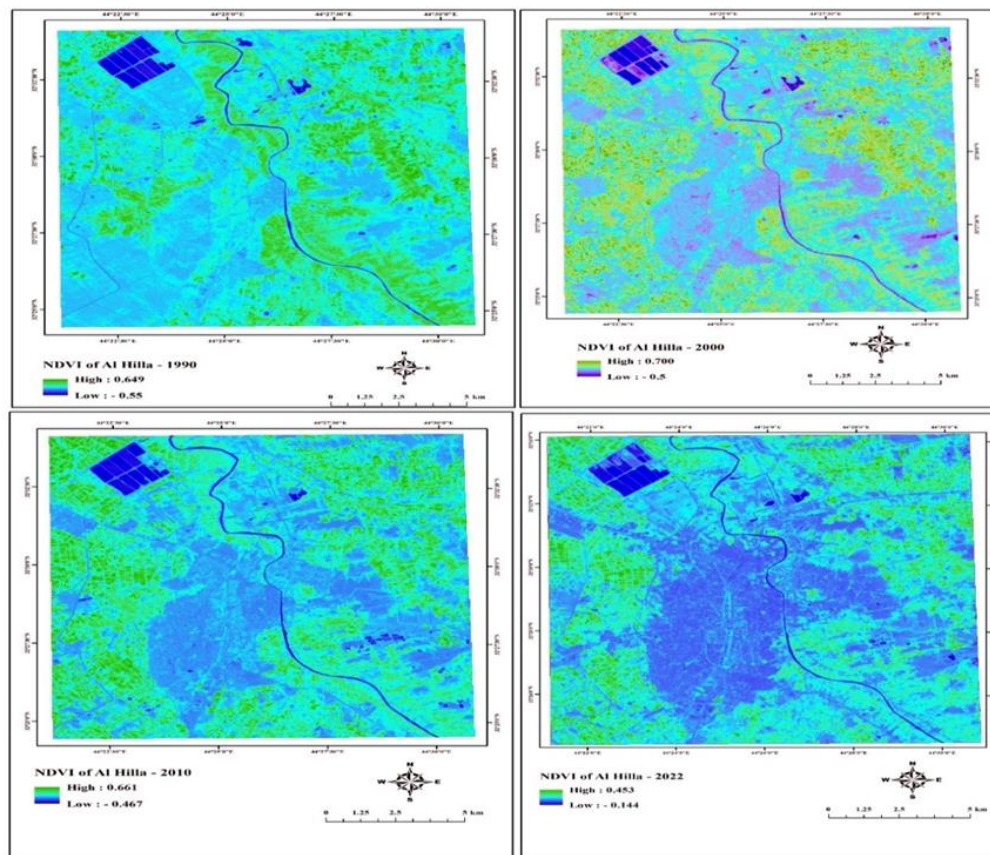


Figure 2: NDVI of Al-Hillah.

A wide vegetation cover of 0.70 was achieved through palm trees and plantations that spread on the land on both sides of the Euphrates River. This is an increase in the percentage of NDVI during the period (1990-2000) by 5%, due to the increase in the expansion of agricultural lands at the expense of arid areas to comply with urban planning standards. Whereas, 0.70 is the NDVI ratio, which is represented by palm trees and plants scattered in the land on both sides of the Euphrates River and modern agricultural areas.

In 2010, the NDVI scale of the Landsat 5 image was between (0.66 - 0.46). A wide vegetation cover of 0.66, the percentage of NDVI decreased in some areas of Al-Hillah, as well as with regards to the orchards spread on both sides of the Euphrates River for several reasons, including drought and weak management and the most important reasons, is the weakness of the system which caused a decrease in the water level compared to the previous years. This is what became clear in classification of aerial photographs, as these reasons helped land owners manipulate and turn them into vacant lands, and some of them turned into residential areas.

Considering that this time period was characterized by an increase in residential and commercial areas and a decrease in green areas, the results were reached in 2010 (0.66 - 0.46). A significant decrease was observed in many agricultural lands and orchards on both sides of the Euphrates in 2022, according to Landsat 8 OLI, which was in the range (0.45-0.14). This is due to a number of factors, including drought and the conversion of these areas into residential or arid areas. In addition, the urban area of Al-Hillah has grown to better accommodate population growth. These are the reasons for the decline in vegetation cover in Al-Hillah and a sharp decrease in the area of green spaces in 2022.

4.2. NDWI

The results of the NDWI were conducted during the years of study in Al-Hillah city. The analysis of Landsat 5 TM images for the year 1990 revealed that the NDWI values during this period were (0.60 - 0.55), and it became clear in this year that the highest NDWI ratio was 0.60 and the lowest ratio was -0.55. These ratios of the NDWI index are represented in the Euphrates River and other rivers and lakes in Al-Hillah for the year 1990.

In 2000, the NDWI scale of the Landsat 5 image was between (0.61 - 0.61) it became clear because there was a slight increase in the value of the NDWI index by 1%, due to the stability of the climate during this period.

NDWI results were also conducted during the study years in Al-Hillah city. Analysis of Landsat 5 TM images for the year 2010 revealed that the NDWI values during this period were (0.56 - 0.57). The NDWI value decreased as a result of climate change and rising temperatures. The reason is also due to drought and desertification, which caused a reduction in water levels and a decrease in rainfall rates.

A significant decrease (0.18 - 0.39) in the level of the Euphrates, water bodies and artificial streams was observed in 2022, according to the NDWI ratio measured by the classification of aerial images of the Landsat 8 OLI satellite. The city of Al-Hillah witnessed huge fluctuations in water, because this city turns into barren lands and some of them into residential cities as a result of the increase in population and urban expansion, as well as a result of high temperatures and climate change that led to a high rate of evaporation. The NDWI values indicated that the water levels decreased due to the decrease in rainfall and the level of rivers compared to previous years which led to the drying of areas far from the center of the city, as shown in the Fig. 3.

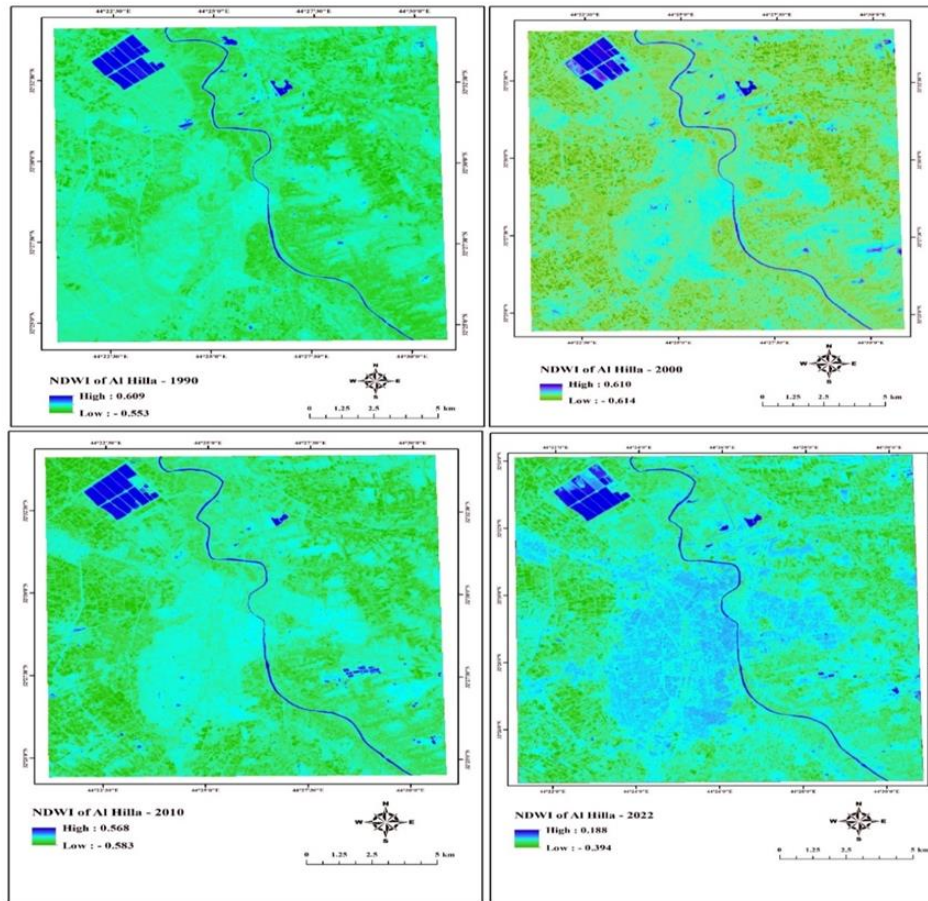


Figure 3: NDWI of Al-Hillah.

4.3. LULC

The results of LULC show an obvious disparity in the Landsat images in 1990, 2000, 2010, and 2022 for Al-Hillah city. In 1990, the results showed that the water area was about 8.7 km^2 , represented by the Euphrates River, artificial lakes and rivers (Fig. 4). The results of year 2000 showed that the water area was about 7.9 km^2 , the agricultural, grassland, and orchard area were 79.7 km^2 and the dry regions covered 160 km^2 . The area of residential was 22.8 km^2 . For 2010, the results showed that the water area was about 12.6 km^2 , with agricultural, grassland, and orchard area of 128.6 km^2 . The dry regions covered 78.3 km^2 and the residential area was 50.5 km^2 .

The results of 2022 showed that the water area is 15.7 km^2 with agricultural, grassland, and orchard area 75.5 km^2 and the dry regions covered 122 km^2 . Additionally, 57 km^2 of residential space was present and arid areas decreased due to the shifting in the residential areas.

Fig. 5 shows a comparison of LULC for the city of Al-Hillah obtained using Landsat 5 TM for the period 1990-2000-2010, and Landsat 8 OLI in 2022. On the contrary, the increase in residential areas and urbanization during 2022 led to a decrease in orchards, lawns, gardens, and even arid areas.

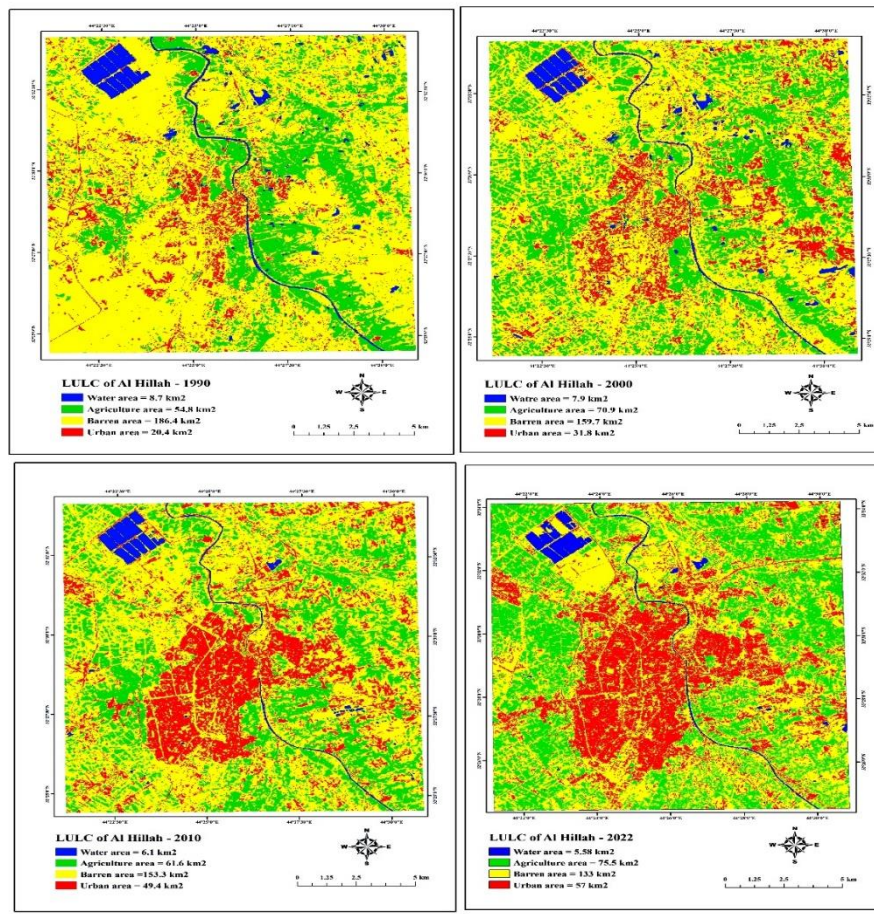


Figure 4: LULC of Al-Hillah.

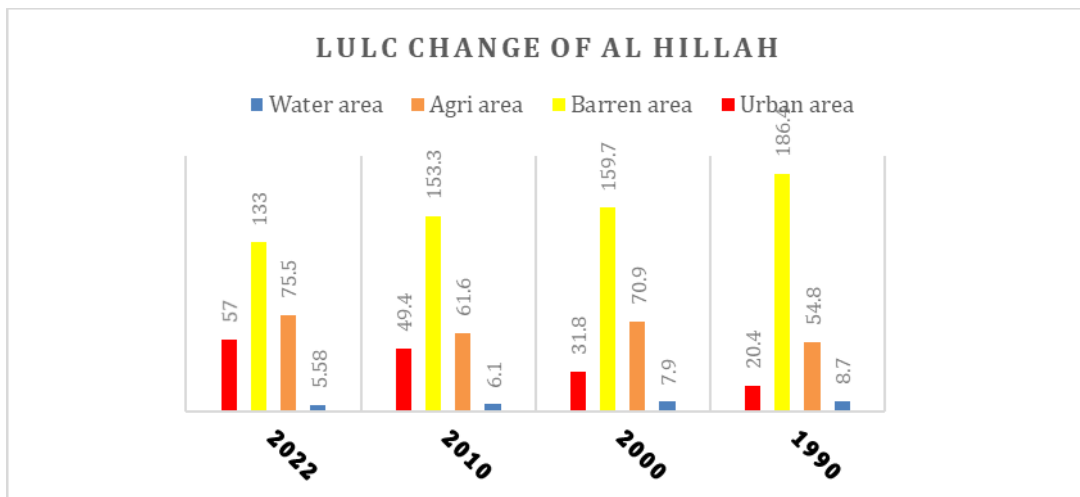


Figure 5: Comparison between areas of LULC classes in Al-Hillah.

5. Discussion

Al-Hillah city is the center of Babylon province, and one of agricultural regions in Iraq. The current study included calculation of NDVI, NDWI and LULC classifications based on Landsat 5 TM and Landsat 8 OLI images obtained in 1990, 2000, 2010, and 2022. The results showed there is an apparent expansion in urban areas from 20.4 km² in 1990 to reach about 57 km² in 2022. On the other hand, there was a decrease in some of the areas of Al-Hillah, with regards to the orchards spread on both sides of the Euphrates River for several reasons, such as drought and government policy according to classification of image during 1990-2022. While barren area declined from 186.4 km²

to 133 km² in 2022, the reason is due to the increase in the pattern urbanization and population expansion at the expense of empty areas. The large urban expansion in the city of Al-Hillah during the current study reflects the clear population increase in Iraq in recent years [52]. This led to an increase in the urban area in city centers, including Al-Hillah, at the expense of barren areas. In addition, urban expansion will put pressure on agricultural areas in the future to accommodate the expected population increase. The change in land use affects the amount of water, so it increases and decreases according to the use.

6. Conclusions

This study proves that the recent developments in remote sensing techniques and GIS provide a powerful tool for mapping and detecting changes in NDVI, NDWI, and LULC. The results of the NDVI, NDWI, and LULC analyses in the current study showed that the dominant characteristic of Al-Hillah city was the urban areas that expanded gradually during the 32 years from 1990-2022. However, there was a slight increase in water and agricultural areas. The continuous urban expansion led to a reduction in barren areas in favor of urban areas. Urban planning for a long period of time, which is based on LULC analysis, where demographic changes greatly affected land use in the city of Al-Hillah, and the increase appears significantly in the urban and residential areas. With regard to undesirable changes in land use and the need for better sustainable development in the city, we therefore suggest that the government reconsider the policies that apply to the area, as well as the policies of the surrounding areas that directly or indirectly affect the development of the study area.

Acknowledgements

The authors would like to thank the University of Baghdad, College of Science, Department of Remote Sensing for their assistance in carrying out this work.

Conflict of interest

Authors declare that they have no conflict of interest.

References

1. A. I. Hamad, A. B. Ali, and A. F. Hassoon, in AIP Conference Proceedings (AIP Publishing, 2022). p.
2. M. Hussain, D. Chen, A. Cheng, H. Wei, and D. Stanley, *SPRS J. Photogram. Rem. Sens.* **80**, 91 (2013).
3. F. K. M. Al Ramahi, M. S. Jasim, and M. J. Rasheed, *Eco. Envir. Conser.* **26**, 446 (2020).
4. O. O. Othow, S. L. Gebre, and D. O. Gameda, *J. Rem. Sens. GIS* **6**, 218 (2017).
5. A. Mustafa and M. Szydłowski, *Rem. Sens.* **12**, 1302 (2020).
6. A. Al-Bayati and S. Jabbar, in IOP Conference Series: Earth and Environmental Science (IOP Publishing, 2021). p. 012039.
7. M. Allawai and B. Ahmed, in IOP conference series: materials science and engineering (IOP Publishing, 2020). p. 012062.
8. F. K. M. Al-Ramahi, M. H. Hasan, and A. A. Zaeen, *Iraqi J. Sci.* **63**, 3236 (2022).
9. S. A. Salleh, Z. A. Latif, W. M. N. W. Mohd, and A. Chan, *Proce. Soci. Behav. Sci.* **105**, 840 (2013).
10. J. A. Richards and J. A. Richards, *Remote Sensing Digital Image Analysis* (Verlag Berlin Heidelberg, Germany, Springer, 2022).
11. C. Oppenheimer, *Geo. Mag.* **136**, 213 (1999).

12. A. A. Aleissae, A. Kumar, R. M. Anwer, S. Khan, H. Cholakkal, G.-S. Xia, and F. S. Khan, *Rem. Sens.* **15**, 1860 (2023).
13. A. K. M. Ali, F. K. M. Al-Ramahi, and A.-R. B. Ali, *Eco. Env. Cons.* **25**, S44 (2019).
14. B. Abdulrahman, K. Fouad, and N. Sabah, *Indian J. Nat. Sci.* **8**, 14215 (2018).
15. F. K. Mashee, O. H. Mutlag, and M. J. Rasheed, *Eur. Asian J. Bio. Sci.* **14**, 3367 (2020).
16. F. K. M. Al-Ramahi, S. B. Mohammed, and M. H. Hasan, in *IOP Conference Series: Earth and Environmental Science* (IOP Publishing, 2023). p. 012020.
17. F. K. M. Al Ramahi and Z. K. I. Al Bahadly, *Baghdad Sci. J.* **17**, 126 (2020).
18. O. Lang, Y. Gandelsman, M. Yarom, Y. Wald, G. Elidan, A. Hassidim, W. T. Freeman, P. Isola, A. Globerson, and M. Irani, in *Proceedings of the IEEE/CVF International Conference on Computer Vision* (Notre Dame, Indiana Computer Vision Foundation, 2021). p. 693.
19. Z. Abbas and H. S. Jaber, in *IOP Conference Series: Materials Science and Engineering* (Iop Publishing, 2020). p. 012166.
20. I. M. Mohammed Irzoqy, L. F. Ibrahim, and H. M. A. Al-Tufaily, in *IOP Conference Series: Earth and Environmental Science* (IOP Publishing, 2022). p. 012010.
21. K. H. Fahad, S. Hussein, and H. Dibs, in *IOP conference series: materials science and engineering* (IOP Publishing, 2020). p. 012046.
22. Congress. *United States Geology Survey (USGS)*; <http://earthexolorer.usgs.gov>.
23. J. W. Rouse, R. H. Haas, J. A. Schell, and D. W. Deering, *NASA Spec. Publ.* **351**, 309 (1974).
24. M. J. Rasheed and F. K. M. Al-Ramahi, *Iraqi Geo. J.* **54**, 69 (2021).
25. B. M. Hashim, A. Al Maliki, M. A. Sultan, S. Shahid, and Z. M. Yaseen, *Nat. Haz.* **112**, 1223 (2022).
26. N. Blagojević, S. Brzev, M. Petrović, J. Borozan, B. Bulajić, M. Marinković, M. Hadzima-Nyarko, V. Koković, and B. Stojadinović, *Bull. Earthq. Eng.* **21**, 1 (2023).
27. M. Stanny, Ł. Komorowski, and A. Rosner, *Energies* **14**, 5030 (2021).
28. J. A. Richards, *Remote Sensing Digital Image Analysis* (Berlin/Heidelberg, Germany, Springer, 2022).
29. A. Velastegui-Montoya, P. Escandón-Panchana, G. Peña-Villacreses, and G. Herrera-Franco, *Clean. Eng. Tech.* **15**, 100659 (2023).
30. R. Neware, *Envir. Earth Sci. Rem. Sens.* **1**, 2019030122 (2019).
31. G. Zhu, X. Liu, and Z. Jia, in *Multiple Representation and Interoperability of Spatial Data* (Hanover, Germany ISPRS, 2006). p. 22.
32. A. Rahman, S. Kumar, S. Fazal, and M. A. Siddiqui, *J. Indian Soci. Rem. Sens.* **40**, 689 (2012).
33. D. Erasu, *J. Rem. Sens. GIS* **6**, 5 (2017).
34. B. L. Decost and E. A. Holm, *Comput. Mat. Sci.* **110**, 126 (2015).
35. M. Alam, D. Le, J. I. Lim, R. V. Chan, and X. Yao, *J. Clin. Medic.* **8**, 872 (2019).
36. K. Salman and B. A. Al Razaq, *Iraqi J. Phys.* **21**, 60 (2023).
37. B. S. Ismael, B. A. Alazaq, Z. F. Rasheed, and E. F. Khanjer, *Indian J. Nat. Sci.* **9**, 15521 (2018).
38. H. Aghsaei, N. M. Dinan, A. Moridi, Z. Asadolahi, M. Delavar, N. Fohrer, and P. D. Wagner, *Sci. Tot. Envir.* **712**, 136449 (2020).
39. C. V. Sudhakar and G. U. Reddy, *Int. J. Intel. Sys. Appl. Eng.* **10**, 75 (2022).
40. F. Belete, M. Maryo, and A. Teka, *Int. J. River Basin Manag.* **21**, 211 (2023).
41. A. Basnet and D. B. Khadka, *GSJ* **8**, 534 (2020).

42. F. F. Sabins Jr and J. M. Ellis, *Remote Sensing: Principles, Interpretation, and Applications* (Long Grove, Illinois, Waveland Press, 2020).
43. T. A. Dhamin, E. Khanjer, and F. Mashee, *MINAR Int. J. Appl. Sci. Tech.* **2**, 57 (2020).
44. N. K. Ghazal, A. H. Shaban, F. K. Mashi, and A. M. Raihan, *Iraqi J. Sci.* **53**, 950 (2012).
45. S. Kumar, S. Arya, and K. Jain, *Int. J. Info. Tech.* **14**, 2035 (2022).
46. M. K. I. Muhammad, S. Shahid, T. Ismail, S. Harun, O. Kisi, and Z. M. Yaseen, *Theo. Appl. Clim.* **144**, 1419 (2021).
47. B. M. Hashim, M. A. Sultan, M. N. Attyia, A. A. Al Maliki, and N. Al-Ansari, *Appl. Sci.* **9**, 2016 (2019).
48. S. K. Mcfeeters, *Int. J. Rem. Sens.* **17**, 1425 (1996).
49. C. Huang, Y. Chen, S. Zhang, and J. Wu, *Rev. Geophys.* **56**, 333 (2018).
50. B. Haxhismajli, E. Hajrizi, and B. Qehaja, in *2022 29th International Conference on Systems, Signals and Image Processing (IWSSIP)* (IEEE, 2022). p. 1.
51. A. S. J. I. J. O. S. Mahdi, *Iraqi J. Sci.* **63**, 4609 (2022).
52. S. S. Rwanga and J. M. Ndambuki, *Int. J. Geosci.* **8**, 611 (2017).

تقييم التوسع العمراني المستدام مع استخدامات الأراضي وتغيرات الغطاء الأرضي لمدينة الحلة باستخدام تقنيات الاستشعار عن بعد ونظم المعلومات الجغرافية

سيف سلام¹، سندس عبد العباس¹ و باسم محمد²
¹قسم التحسس النائي، كلية العلوم، جامعة بغداد، بغداد، العراق
²وزارة العلوم والتكنولوجيا، دائرة البيئة والمياه، بغداد، العراق

الخلاصة

في الدراسة الحالية، تم استخدام بيانات الأقمار الصناعية ونظام المعلومات الجغرافية (GIS) للكشف عن التغيير في استخدام الأراضي / الغطاء الأرضي (LULC) في مدينة الحلة، وسط العراق خلال الفترة 1990 - 2022. تهدف الدراسة إلى حساب NDVI و NDWI و LULC في الحلة باستخدام صور Landsat 5 TM و Landsat 8 OLI وأظهرت النتائج أن هناك توسعاً ظاهرياً في المنطقة العمرانية من 20.5 كم² عام 1990 إلى حوالي 57 كم² عام 2022. ومن ناحية أخرى أظهرت النتائج أن هناك زيادة طفيفة في المساحات الزراعية والمياه. بينما انخفضت المساحة القاحلة من 168.7 كم² إلى 122 كم² في عام 2022. التخطيط الحضري طويل الأجل، الذي يعتمد على تحليل LULC هو أداة فعالة لصناع القرار لدراسة الأنماط المستقبلية في التوسع الحضري بالتوازي مع الارتفاع المتوقع من سكان العراق في السنوات القادمة. في حين حدثت زيادة طفيفة في المساحات المائية والزراعية. وأدى التوسع العمراني المستمر إلى تقليص المناطق القاحلة لصالح المناطق الحضرية. التخطيط العمراني لفترة طويلة من الزمن، والذي يعتمد على تحليل LULC حيث أثرت التغيرات الديموغرافية بشكل كبير على استخدام الأراضي في مدينة الحلة، وتظهر الزيادة بشكل كبير في المناطق الحضرية والسكنية.

الكلمات المفتاحية: التوسع العمراني، استخدامات الأراضي، الغطاء الأرضي، نظم المعلومات الجغرافية، بيانات لاندسات.